Available online at www.sciencedirect.com
ScienceDirect
Journal of Power Sources 176 (2008) 381–386
JOURNAL OF POWER SOURCES
www.elsevier.com/locate/jpowsour

Short communication

A study of the Al content impact on the properties of $MmNi_{4.4-x}Co_{0.6}Al_x$ alloys as precursors for negative electrodes in NiMH batteries

S. Bliznakov [a,b,*], E. Lefterova [a], N. Dimitrov [b], K. Petrov [a], A. Popov [a]

[a] *Institute of Electrochemistry and Energy Systems, Bulgarian Academy of Sciences, Acad. G. Bonchev Street, Block 10, 1113 Sofia, Bulgaria*
[b] *Department of Chemistry, State University of New York at Binghamton, P.O. Box 6000, Binghamton, NY 13902-6000, United States*

Received 6 September 2007; received in revised form 10 October 2007; accepted 11 October 2007
Available online 18 October 2007

Abstract

AB_5-type hydrogen storage alloys with $MmNi_{4.4-x}Co_{0.6}Al_x$ (Mm-mischmetal) composition are synthesized, structurally and thermodynamically characterized, and electrochemically tested in 6 M KOH electrolyte. It is shown that an increase of the Al content in the alloy results in expansion of both the alloy lattice cell size and the unit cell volume. These structural changes lead to decrease of the plateau pressure and increase of the plateau width in the pressure-composition-temperature desorption isotherms. Improvement of the specific electrode capacity is also registered with the increase of the cell parameters. In addition to that the higher Al content is found to enhance the stability of the alloy components' hydrides. Maximum discharge capacity of 278 mAh g^{-1} is measured with an electrode made from a $MmNi_{3.6}Co_{0.6}Al_{0.8}$ alloy. Cycle life tests of the accordingly prepared electrodes suggest a stability that is comparable to the stability of commercially available hydrogen storage electrodes.

Keywords: AB_5 hydrogen storage alloys; MH electrodes; Rechargeable Ni/MH batteries

1. Introduction

Multicomponent hydrogen storage alloys have been used as a negative electrode material in commercialized nickel/metal hydride (NiMH) rechargeable batteries since 1990 [1–3]. At present, there are more than 2700 hydrogen storage materials [4,5] that are known to reversibly absorb hydrogen at different pressures and temperatures. However, only a few types of hydrogen storage alloys comply with the requirements for electrochemical applications. Although numerous hydrogen storage alloys have been studied for possible electrochemical applications for the last three decades, only two alloy types, AB_5-type ($LaNi_5$) and AB_2-type (ZrV_2), have been used as precursors for MH negative electrodes fabrication [3]. It is shown in recent papers [4–6] that partial substitution and/or small addition of other elements for both A and B components in the stoichiometric AB_5- and AB_2-type compounds could change their key characteristics: (i) crystal lattice constants and unit cell volume, (ii) hydrogen absorption/desorption equilibrium pressure, (iii) hysteresis between hydrogen absorption/desorption plateaus, (iv) kinetics of hydriding/dehydriding reactions, and (v) alloys stability (by preventing oxide formation of one or more of the components). Also, such substituted $MmNi_5$ alloy is considerably less expensive than $LaNi_5$, and yet it absorbs identical or higher amount of hydrogen [7]. However, the disadvantage for possible electrochemical applications of $MmNi_5$ is its very high equilibrium hydrogen desorption pressure at ambient temperature (2.3 MPa) [5].

According to earlier studies a remedy for this could be a partial replacement of Ni by other metals (such as Co, Al, Mn, Cr, Fe, Sn, etc., or a combination of these metals) that generally would improve the sorption properties of $MmNi_5$ [5,8]. This is supported by the fact that mainly the AB_5-type alloy with composition $MmNi_{3.55}Mn_{0.4}Al_{0.3}Co_{0.75}$ has so far been used in industrial applications [3]. The electrochemical capacity decay with the number of charge/discharge cycles of AB_5-type electrodes is associated mainly with surface passivation. It is believed that such passivation is due to oxidation and pulverization of alloy particles resulting from repetitive volume changes during the hydrogen absorption/desorption process [9].

* Corresponding author at: Department of Chemistry, State University of New York at Binghamton, P.O. Box 6000, Binghamton, NY 13902-6000, United States. Tel.: +1 607 777 7949; fax: +1 607 777 4478.
E-mail address: sbliznak@binghamton.edu (S. Bliznakov).

0378-7753/$ – see front matter © 2007 Elsevier B.V. All rights reserved.
doi:10.1016/j.jpowsour.2007.10.028

Also, the influence of rare earth content on the electrochemical hydrogen storage properties of $MmNi_{3.5}Mn_{0.4}Al_{0.3}Co_{0.8}$ alloy was recently investigated [9] and a maximum discharge capacity in the range of 179–266 mAh g^{-1} was reported for La/Ce (ratio in the range of 0.51–18.73, the optimum ratio La/Ce is 12) alloy electrodes. Other authors, Wei et al. [10], investigated hypo-stoichiometric AB_5 alloys with compositions $Mm(Ni_{3.55}Co_{0.75}Mn_{0.4}Al_{0.3})_{5x}$ ($x = 0.88$, 0.92, 0.96, and 1) and reported that the maximum discharge capacity first increased from 305 mAh g^{-1} ($x = 0.88$) to 332 mAh g^{-1} ($x = 0.96$) and then decreased back to 320 mAh g^{-1} ($x = 1$). The electrochemical properties of low cost $MmNi_5$-based hydrogen storage alloys are extensively examined in Ref. [11]. It is found that $MmNi_{3.5}Co_{0.7}Al_{0.8}$ alloy showed very long cycle life with reasonable discharge capacity (250 mAh g^{-1}) and rate capability [11]. Thus, the decay in the MH capacity electrode in this case is only 10% after 2000 cycles.

Key requirements for battery application of MH alloys are associated with stability over a large number of charge–discharge cycles, high sorption capacity, suitable thermodynamic properties for a reversible hydrogen absorption/desorption (the heat of hydride formation/decomposition value should range between −15 and −50 kJ mol^{-1}), low hydrogen equilibrium pressure (between 0.001 and 0.1 MPa), favorable kinetic properties for high-rate performance, high oxidation resistance, and low cost [4].

The above discussion along with the drive toward commercialization of NiMH batteries that would be competitive with Li-ion batteries clearly suggest the necessity of development of new advanced MH alloys that would feature higher energy density, faster activation, better dischargeability, and lower cost. In addition to that, an improvement of the electrode preparation technology is needed for the development of high power density energy sources for portable electronics, electric and hybrid vehicles, and emergency applications [4,6]. In response to all that, this paper is aimed at comprehensively studying the influence of the Al content in AB_5-type $MmNi_{4.4-x}Co_{0.6}Al_x$ alloys on their structure, hydrogen desorption thermodynamics and electrochemical properties. The work herein emphasises three distinct experimental components as follows: (i) synthesis of alloys with composition $MmNi_{4.4-x}Co_{0.6}Al_x$ ($x = 0$, 0.3, 0.4, 0.5, 0.6, 0.8, and 1); (ii) investigation of the alloy structure and its impact on the thermodynamics of the hydriding/dehydriding process from gas phase; (iii) electrochemical characterization of electrodes prepared from selected alloys, with regard to their possible application in Ni/MH batteries.

2. Experimental

A semi-industrial, high frequency vacuum inductive melting/annealing apparatus was used for the alloy synthesis. The mischmetal (Mm) consisted of 52 wt.% La, 33 wt.% Ce, 4 wt.% Pr, and 11 wt.% Nd. Annealing in high purity Ar atmosphere for 4 h at 950 °C was applied just after the melting process, followed by mechanical milling. The crystal structure and the alloy phases were studied by X-ray diffraction using Philips-APD 15 powder diffractometer with Cu Kα radiation. The X-ray spectra of three diffraction peaks (between 58° and 65° 2Θ) for structural characterization were registered by applying a step scanning with increments of 0.02° 2Θ and sampling time of 1 s. The hydrogen absorption/desorption properties of the alloys from gas phase were studied by an automated Sieverts type apparatus for investigation of hydrogen absorption/desorption in intermetallic compounds [12]. The desorption pressure-composition-temperature (PCT) isotherms were measured at hydrogen pressure of 0.1–1 MPa in the temperature range of 313.15–353.15 K. Prior to PCT measurements the samples were activated by hydrogen at a pressure of 2.5 MPa and three absorption/desorption cycles were then typically performed for each sample.

Two non-sintered techniques for working electrode preparation were used. The first one (#1) included preparation of a slurry with weight ratio of alloy powder:graphyte:(PTFE emulsion) = 92:5:3 followed by drying in a furnace and pressing in 1 cm^2 matrix under pressure of 19.62 MPa from both sides of a current collector (Ni-mesh) at ambient temperature. The second technique (#2) comprised homogenization of a mixture that consisted of alloy and preliminary teflonized (20 wt.%) carbon black (Vulcan 72®) followed by pressing in the matrix at conditions described in technique #1. It has been shown that Vulcan XC-72 has unique suitability for carrier in MH alloy electrodes that is manifested by long cycle life and high discharge capacity in standard electrochemical tests [13]. All electrochemical measurements in this work were conducted in a conventional three-electrode cell at ambient temperature, using 6 M KOH as working electrolyte. A large surface area Ni-foam served as counter electrode. All potentials were measured and quoted versus Hg/HgO reference electrode. Charge/discharge cycles in galvanostatic mode were carried out by a three-channel, software controlled, home-made galvanostat, developed in IEES-Bulgarian Academy of Sciences. The electrodes were charged for 4.5 h at a current density of 100 mA g^{-1} and discharged at 50 mA g^{-1} to a cutoff potential of −0.6 V.

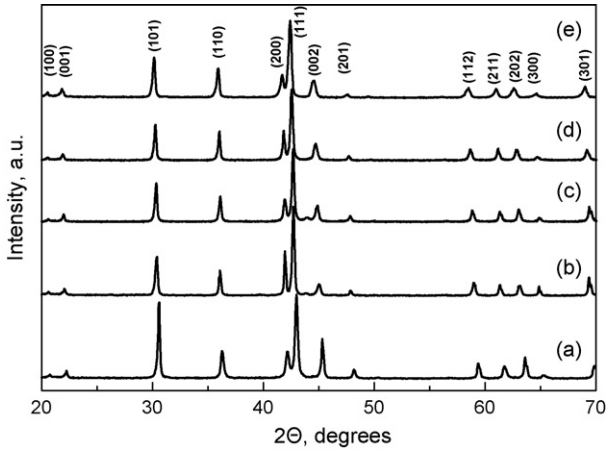

Fig. 1. XRD spectra of $MmNi_{4.4-x}Co_{0.6}Al_x$ alloys: (a) $x = 0$; (b) $x = 0.5$; (c) $x = 0.6$; (d) $x = 0.8$; (e) $x = 1$.

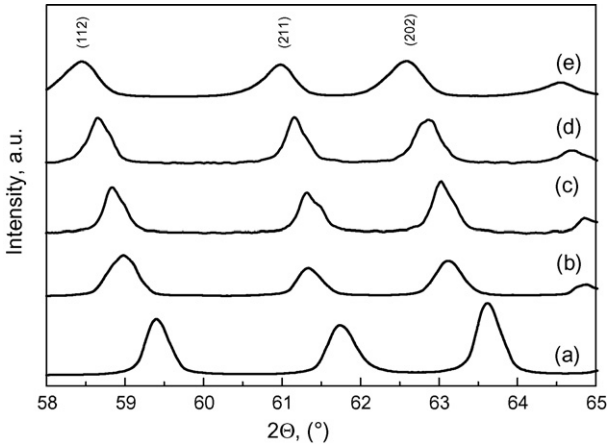

Fig. 2. XRD spectra of the $MmNi_{4.4-x}Co_{0.6}Al_x$ alloys with a scan rate of 0.02 $2\Theta\ s^{-1}$ and sampling time of 1 s: (a) $x=0$; (b) $x=0.5$; (c) $x=0.6$; (d) $x=0.8$; (e) $x=1$.

3. Results and discussion

3.1. Structural analysis

The X-ray spectra of $MmNi_{4.4-x}Co_{0.6}Al_x$ alloys synthesized by the above-described vacuum induction melting method are presented in Fig. 1. A phase with hexagonal $CaCu_5$-type lattice that corresponds to $LaNi_5$ intermetallic compound is identified. Diffraction peaks of other phases or of plain metals are not observed. This proves that the component mixing during the melting process is fully completed. The characteristic (1 1 2), (2 1 1), and (2 0 2) diffraction peaks of the same samples are shown as collected at higher magnification increments of 0.02° 2Θ and sampling time of 1 s in Fig. 2. It could be seen that an increase of the Al content leads to both: (i) increase of the peak width and (ii) peak shift toward lower angles. The peak width increase could be due to a grain size decrease as well as to an accumulation of additional strains, presence of inhomogeneties and/or microsegregations. The lower angle shifted peaks are apparently associated with an increase of the inter-planar distance in the crystal lattice and respectively with an increase of the unit cell parameters. This in turn leads to an increase of the unit cell volume as summarized in Table 1.

Table 1
Cell parameters and unit cell volumes of $MmNi_{4.4-x}Co_{0.6}Al_x$ alloys synthesized in this work

Composition of the alloy	Cell parameters (Å)		Unit cell volume (Å^3)
	a	*c*	
$MmNi_{4.4}Co_{0.6}$	4.946	4.001	84.763
$MmNi_{3.9}Co_{0.6}Al_{0.5}$	4.976	4.022	86.283
$MmNi_{3.8}Co_{0.6}Al_{0.6}$	4.979	4.041	86.756
$MmNi_{3.6}Co_{0.6}Al_{0.8}$	4.991	4.056	87.499
$MmNi_{3.4}Co_{0.6}Al$	5.000	4.069	88.116

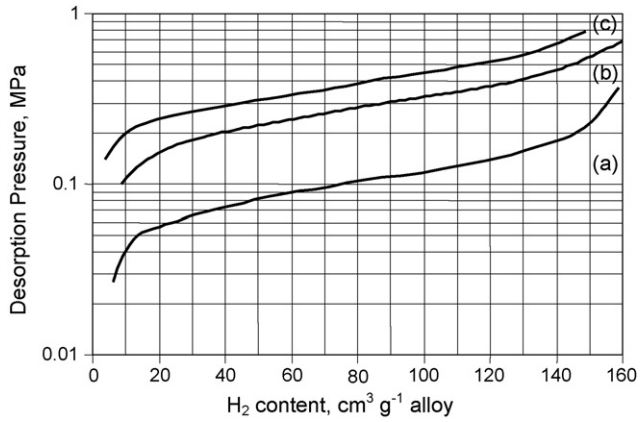

Fig. 3. Hydrogen desorption isotherms of $MmNi_{4.0}Co_{0.6}Al_{0.4}$ alloy at different temperatures: (a) $T=313.15$ K; (b) $T=338.15$ K; (c) $T=348.15$ K.

3.2. Analysis of PCT isotherms

The desorption isotherms obtained with $MmNi_{4.0}Co_{0.6}Al_{0.4}$ alloy at 313.15, 338.15, and 348.15 K are presented in Fig. 3, where the hydrogen desorption pressure is plotted as a function of the amount of desorbed hydrogen. It is seen that the equilibrium pressure increases with temperature as illustrated by measured values of 0.1 MPa at 313.15 K to 0.4 MPa at 348.15 K. The highest amount of desorbed hydrogen in these experiments is found to be 160 $cm^3\ g^{-1}$ that in turn yields a capacity of 375 $mAh\ g^{-1}$. This value is fairly close to the theoretically calculated one for $LaNi_5H_6$ (372 $mAh\ g^{-1}$). Additional desorption isotherms registered for the $Mm(NiCo)_{5-x}Al_x$ system at temperatures 338.15 and 348.15 K are also presented in Figs. 4 and 5, respectively. Apparently, the increase of the Al content results in a decrease of the plateau pressure and hence in lower values of the equilibrium pressure. At the same time, the observed increase of the plateau width (as seen in Figs. 4 and 5) could be directly associated with the increase of the amount of reversibly desorbed hydrogen and in turn with the corresponding increase of the electrode capacity.

Fig. 6 represents the immediate relationship between hydrogen desorption pressure and Al content in the alloy at two different temperatures. The results clearly show that alloys with

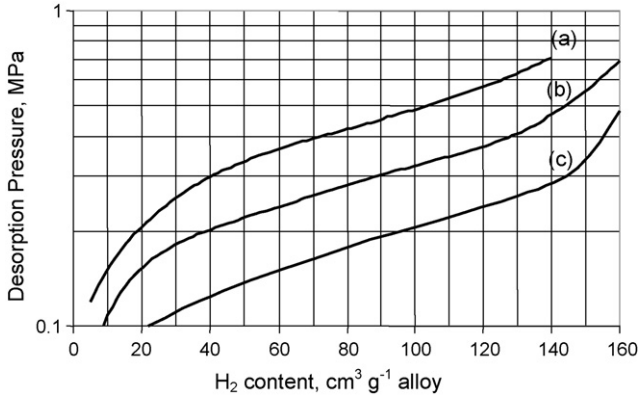

Fig. 4. PCT desorption isotherms at 338.15 K of $MmNi_{4.4-x}Co_{0.6}Al_x$ alloys: (a) $x=0.3$; (b) $x=0.4$; (c) $x=0.5$.

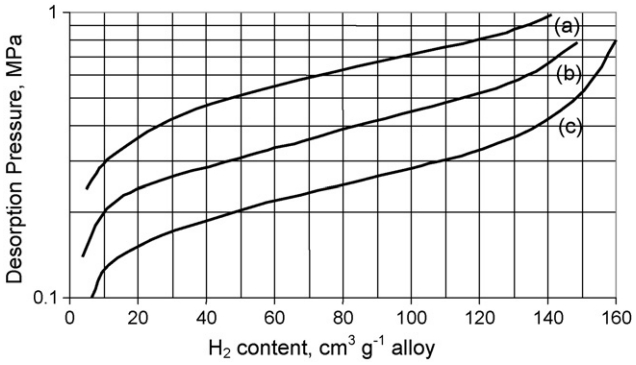

Fig. 5. Hydrogen desorption isotherms at 348.15 K of $MmNi_{4.4-x}Co_{0.6}Al_x$ alloys: (a) $x = 0.3$; (b) $x = 0.4$; (c) $x = 0.5$.

Al content $x > 0.4$ feature desorption pressure below 0.1 MPa at 313.15 K. Knowing that no alloys with desorption pressure above 0.1 MPa at ambient temperature are suitable for electrode application [6], it can be concluded that among the alloys synthesized in this work only those with Al content higher than $x = 0.4$ can be used as negative electrodes. Also, a careful analysis of the PCT isotherms presented in Figs. 3–5 suggests relatively higher values (about 0.56) of the plateau slopes [d ln P/d(H/M)] [5] for Al substituted alloys in comparison with the corresponding ones for $MmNi_5$ alloy (about 0.36) reported in Ref. [5]. This difference could be attributed to metallurgical reasons manifested by the possibility of incorporation into the $MmNi_5$ crystal lattice of Al atoms generated by microsegregation during solidification process. Such incorporation would eventually give raise to a sloping plateau effect.

3.3. Thermodynamic parameters

The relation between equilibrium pressure (P_{eq}), enthalpy (ΔH) and entropy (ΔS) of the hydrogen absorption/desorption reaction is given in thermodynamics by the well-known van't Hoff equation [6,14]. Fig. 7 presents the pressure dependence of the temperature (van't Hoff plots) for some of the studied herein alloys. The enthalpy and entropy changes are calculated

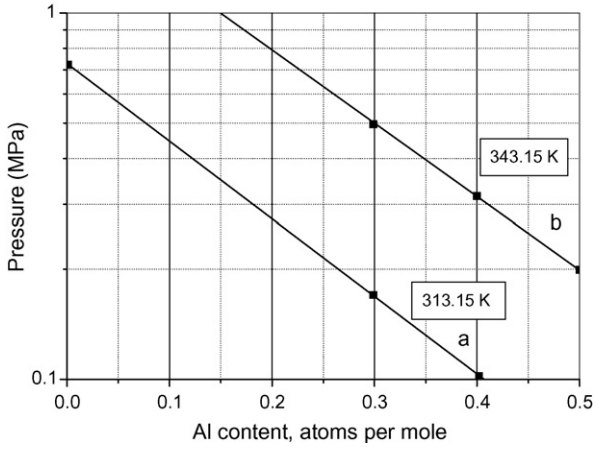

Fig. 6. Dependence of the hydrogen desorption pressure vs. Al content of $MmNi_{4.4-x}Co_{0.6}Al_x$ alloys at: (a) 313.15 K and (b) 343.15 K.

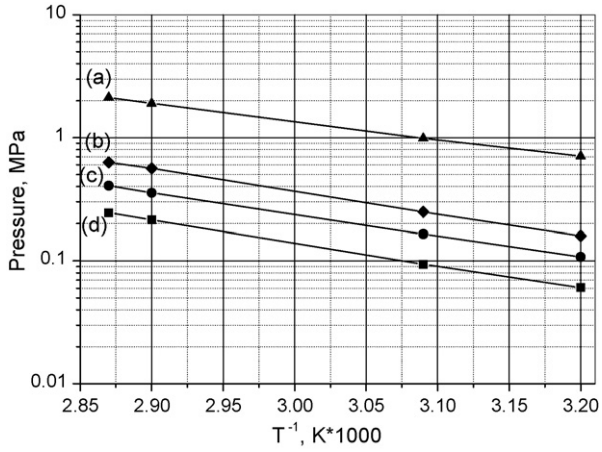

Fig. 7. van't Hoff plots showing the equilibrium pressure as a function of temperature for hydrogen desorption of $MmNi_{4.4-x}Co_{0.6}Al_x$ alloys: (a) $x = 0$; (b) $x = 0.3$; (c) $x = 0.4$; (d) $x = 0.5$.

from the straight-line slopes and intersections with the ordinate axis, respectively. The values of the thermodynamic parameters obtained as a result of these calculations are summarized in Table 2. It is obvious from the data that the absolute value of the alloy enthalpy increases with the Al content increase. This leads to an improved stability of the prepared accordingly hydrides. It is also known that alloys with absolute value of the enthalpy exceeding 50 kJ mol^{-1} are not suitable for electrochemical application as MH electrodes [6,14]. Additional look at Table 2 suggests that according to this criterion only the $MmNi_{3.4}Co_{0.6}Al$ alloy is clearly not suitable for negative electrode material. At the same time presented in Table 2 values of the alloy entropy are generally within the "healthy" range (of order of -130 J mol^{-1} K^{-1}, Ref. [14] for the system hydrogen gas/intermetallic compound.

3.4. Electrochemical characterization

The discharge capacities registered with electrodes, prepared by technique #1 using mischmetal alloys with different Al content ($x = 0.6$ and 0.8) are presented in Fig. 8. From these two, the electrode featuring Al ($x = 0.6$) shows significantly lower capacity. This trend is in good agreement with normally measured changes of the alloy characteristics with increase of the Al content. In this work such changes are manifested by (i) increase of unit cell parameters and unit cell volume (Table 1),

Table 2
Calculated enthalpy and entropy values of $MmNi_{4.4-x}Co_{0.6}Al_x$ alloys synthesized in this work

Alloy type $MmNi_{4.4-x}Co_{0.6}Al_x$	ΔH (kJ mol^{-1})	ΔS (J mol^{-1} K^{-1})
$x = 0.0$	−28.83	−108.45
$x = 0.3$	−32.00	−106.86
$x = 0.4$	−32.34	−104.39
$x = 0.5$	−35.23	−114.09
$x = 0.6$	−41.15	−129.32
$x = 0.8$	−48.40	−132.20
$x = 1.0$	−51.24	−135.40

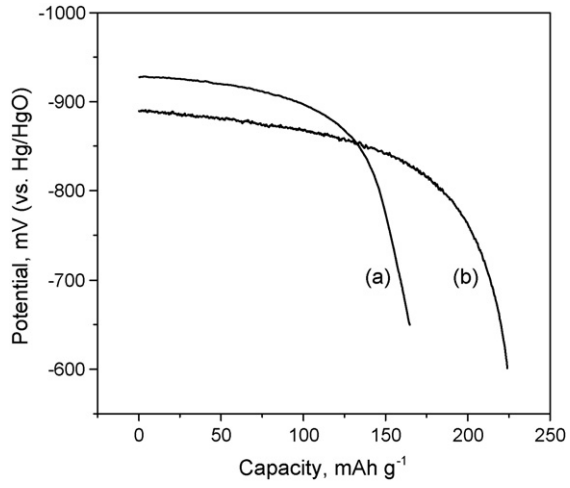

Fig. 8. Discharge curves of the electrodes prepared from $MmNi_{4.4-x}Co_{0.6}Al_x$ alloys by technique #1 at discharge current densities of $i = 50\ mA\ g^{-1}$: (a) $x = 0.6$; (b) $x = 0.8$.

(ii) decrease of plateau pressure and (iii) increase of plateau width, determined from PCT-isotherms (Figs. 4 and 5).

The stability behavior and the rate of dischargeability are key characteristics often used as criteria for their practical applicability as MH electrodes [10]. In the present work, an electrode with composition $MmNi_{3.6}Co_{0.6}Al_{0.8}$ featuring the highest electrochemical discharge capacity and prepared by technique #2 is selected for assessment of these characteristics. The assessment is done by both cycle life-time tests and measurements of the discharge capacity as a function of the discharge current density. The results of preliminary life time tests up to 40 cycles at discharge current density of $50\ mA\ g^{-1}$ are presented in Fig. 9. A maximum discharge capacity of $278\ mAh\ g^{-1}$ is achieved in the 6th charge–discharge cycle. This value is 10–35% higher than the one recently reported for electrodes prepared from AB_5 alloys with similar composition [9,11]. It is also seen that the results in Fig. 9 suggest very fast electrode activation and affirm the expected good stability behavior manifested by a capacity decrease for the duration of the test that is as low as 15%. The discharge curves at six different discharge

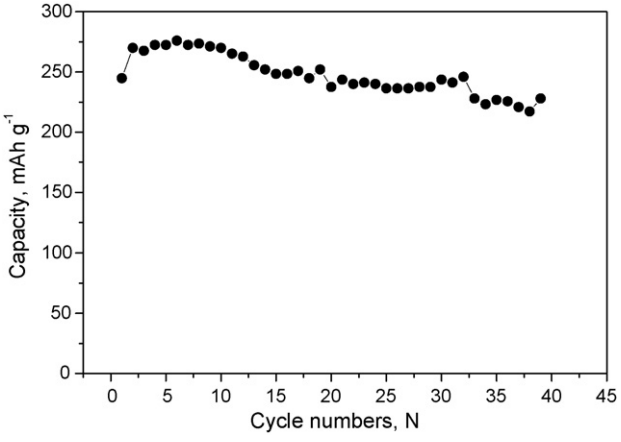

Fig. 9. Cycle life performance of the $MmNi_{3.6}Co_{0.6}Al_{0.8}$ electrode prepared by technique #2 at discharge current densities of $i = 50\ mA\ g^{-1}$.

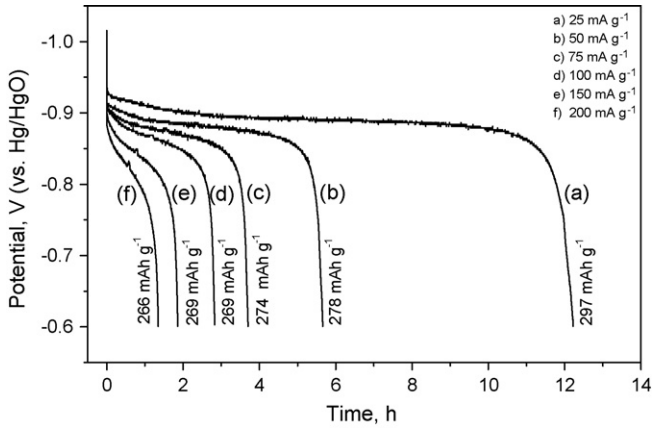

Fig. 10. Discharge curves of $MmNi_{3.6}Co_{0.6}Al_{0.8}$ electrode at different discharge current densities.

current densities registered with $MmNi_{3.6}Co_{0.6}Al_{0.8}$ electrode are presented in Fig. 10. It could be seen that the increase of the discharge current density from 25 to $200\ mA\ g^{-1}$ leads to: (i) increase of the plateau slopes in the discharge curves; (ii) shifting of the discharge plateaus toward lower potentials; (iii) only 10% decrease of the discharge capacity. These results ascertain the outstanding electrochemical behavior and identify the alloy $MmNi_{3.6}Co_{0.6}Al_{0.8}$ as a feasible material for negative MH electrode.

4. Conclusions

A vacuum induction melting method was used for the synthesis of AB_5-type alloys with composition $MmNi_{4.4-x}Co_{0.6}Al_x$ ($x = 0$, 0.3, 0.4, 0.5, 0.6, 0.8, and 1). Structural analysis suggests a hexagonal $CaCu_5$-type crystal lattice for the alloys synthesized in this work. A partial substitution of Ni with $Co_{0.6}$ and Al_x in these alloys was found to result in increase of their lattice cell parameters and unit cell volume.

An increase of the Al content and a temperature decrease were both found to lower the equilibrium pressure of the substituted alloys. At the same time, an enhanced stability of their hydrides is observed with increasing of the Al content. A highest discharge capacity of $278\ mAh\ g^{-1}$ at discharge current density of $50\ mA\ g^{-1}$ was obtained with an $MmNi_{3.6}Co_{0.6}Al_{0.8}$ alloy electrode. The measured value is higher than the ones recently reported in the literature for electrodes prepared from AB_5-type alloys with similar composition. Cycle life tests with electrodes based on $MmNi_{3.6}Co_{0.6}Al_{0.8}$ alloy have shown fairly acceptable stability manifested by a capacity loss of as low as 15% over 40 test cycles. Reasonably high-rate dischargeability resulting in capacity loss of only 10% is seen upon increase of the discharge current density by about an order of magnitude.

In general, the Al substituted MH alloys studied in this work have lower cobalt content which makes them less expensive than the commercially available ones. Also, the outstanding structural, thermodynamical, and electrochemical properties identify the $MmNi_{3.6}Co_{0.6}Al_{0.8}$ alloy synthesized in this work as a strong candidate for negative MH electrode in battery application.

References

[1] T. Sakai, H. Miyamura, N. Kuriyama, H. Ishikawa, I. Uehara, Zietschrift Phys. Chem. 183 (1994) 333–346.

[2] F. Guevas, J. Joubert, M. Latroche, A. Percheron-Guegan, Appl. Phys. A 72 (2001) 225–238.

[3] D. Linden, T. Reddy, Handbook of Batteries, 3rd ed., McGraw-Hill, New York, 2002.

[4] S. Bliznakov, A. Popov, P. Andreev, in: Z. Stoynov, D. Vladikova (Eds.), Portable and Emergency Energy Sources, Prof. Marin Drinov Academic Publishing House, Sofia, 2006, pp. 177–215, ISBN-10:954-322-133-2.

[5] http://hydpark.ca.sandia.gov, metal hydride Internet database, constructed by DOE, International Energy Agency (IEA), and Sandia National Laboratories, September 2007.

[6] J. Kleperis, G. Wojcik, A. Czerwinski, J. Skowronski, M. Kopczyk, M. Beltowska-Brzezinska, J. Solid State Electrochem. 5 (2001) 230.

[7] C.O. Bounds, B.M. Ma, J. Batel, in: R.G. Bautista, C.O. Bounds, T.W. Ellis, B.I. Kilibourn (Eds.), Rare Earths-Science Technology and Applications III, The Minerals, Metals & Materials Society, Orlando, USA, 1997, pp. 87–96, ISBN: 9780873393638.

[8] L.C. Lai, S.Y. Liu, T.P. Perng, in: R.G. Bautista, C.O. Bounds, T.W. Ellis, B.I. Kilibourn (Eds.), Rare Earths-Science Technology and Applications III, The Minerals, Metals & Materials Society, Orlando, USA, 1997, pp. 97–106, ISBN: 9780873393638.

[9] M.V. Ananth, M. Raji, K. Manimaran, G. Balachandran, L.M. Nair, J. Power Sources 167 (2007) 228–233.

[10] G. Wei, H. Shumin, X. Danyang, Li. Yuan, L. Ming, M. Lirong, H. Lin, J. Rare Earths 24 (2006) 227–231.

[11] T. Sakai, H. Yoshinaga, H. Miyamura, N. Kuriyama, H. Ishikawa, J. Alloys Compd. 180 (1992) 37–54.

[12] L. Bozukov, A. Apostolov, T. Mydlarz, J. Magn. Magn. Mater. 83 (1990) 555.

[13] A. Anoni, A. Visintin, K. Petrov, S. Srinivasan, J. Relly, J. Johnson, R. Schwarz, P. Desch, J. Power Sources 47 (1994) 261–275.

[14] D.G. Ivey, D.O. Northwood, J. Mater. Sci. 18 (1983) 321–347.